2009 Second International Conference on Computer and Electrical Engineering

Analysis and Simulation of Speed Control for Two-Mass Resonant System

Ghazanfer Shahgholian
Department of Electrical Engineering Islamic Azad University, Najaf Abad Branch
Esfahan, Iran
shahgholian@iaun.ac.ir

Jawad Faiz
Department of Electrical and Computer Engineering, Faculty of Engineering, University of Tehran
Tehran, Iran
jfaiz@ut.ac.ir

Pegah Shafaghi
Department of Electrical Engineering Islamic Azad University, Najaf Abad Branch
Esfahan, Iran
p_shafaghi@iaun.ac.ir

Abstract— **Torsional vibration suppression and attainment of robustness in motion control systems is a requisite in industry applications. This paper presents the algorithm to design a speed control strategy of a two-mass resonant system by a proportional- integral-derivative (PID) or three-term controller. The simulation results show that the control method has robust stability and fast speed response.**

Keywords- Two-mass system; speed control; coefficient diagram method; modeling.

I. INTRODUCTION

In some industrial applications, like elevators, rolling mill and so on, which has a long shaft and large load side mass or a robot arm which has flexible coupling, the mechanical part of the system has very low resonant frequency. The dynamics of such a system must hence be modeled as a two-mass or multi-mass system. The tasks of the control in the two-mass resonant system are suppress the shaft torsional vibration, reject the effect of the load disturbance torque and tracking the load speed of the speed reference without overshoot [1]. The dynamic performances of speed and position controlled multi-mass driving system can be deteriorated especially due to the elastic coupling, nonlinear friction and backlash. Many methods have been presented in the literature for the torsional vibration control of two-mass system such as time derivative feedback, resonant ratio control, fractional order control, slow resonance ratio control and pole placement [2-7].

The systematic analysis of two-inertia stabilization system in [8] is proposed, and an optimal controller to achieve better reference tracking and disturbance rejection performance is introduced by pole assignment using integral of time multiplied by the absolute error (ITAE) criterion. A novel identification method based on a modified plant instead of the original plant proposed in [9], which applied in the case of a two-mass resonant system, for two different control problems (position control and speed control), in order to evaluate its effectiveness for servo systems. A high-performance speed control for torsional vibration suppression in a two-mass motor drive system by using a Kalman filter and LQ based speed control with an integrator presented in [10]. In the design of a linear time-invariant control system using the classical control theory, the first step is to choose the controller type. In most cases, the cost of control systems increases with its complexity. The conventional PID is widely used in most servo applications such as multi-mass system, robotics, machine tools, and so on. They are easy to adjust and configure, in addition to providing possibilities of improvement in operation and control.

This paper describes a study on the PID controller design of two-mass resonant system considering the response frequency and response step. In section II two-inertia torsional systems used in this paper and in section III the controller to evaluate are presented. In section IV the pole-placement controller such as coefficient diagram method (CDM) is used to assign the closed-loop roots of the system characteristic equation. Simulation results are shown in section V to verify good performance obtained using the proposed speed controller. Then conclusions follow in section VI.

II. TWO-MASS SYSTEM STRUCTURE AND MATHEMATICAL MODEL

The two-mass resonant system consist a motor and a load connected with a flexible shaft is show in Fig.1. The system parameters used in this paper are listed on Table I.

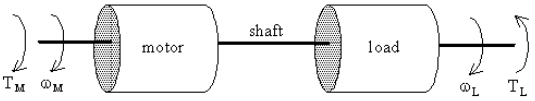

Figure 1. General configuration of the two-mass resonant system

TABLE I. NOMINAL PARAMETERS OF THE TWO-MASS PLANT

Symbol	Quantity	Value
K_S	shaft stiffness	242 Nm/rad
B_S	shaft damping coefficient	15×10^{-2} Nm/rad/s
J_M	motor inertia	6.41×10^{-2} kg.m^2
B_M	coefficient of motor viscosity	2.1×10^{-3} Nm/rad/s
J_L	load inertia	5.23×10^{-2} kg.m^2
B_L	coefficient of load viscosity	5.3×10^{-2} Nm/rad/s

978-0-7695-3925-6/09 $26.00 © 2009 IEEE
DOI 10.1109/ICCEE.2009.41

The state equation of the two-mass resonant system is written in the linear time invariant form:

$$\begin{cases} \dot{X} = A X + B X \\ Y = C X + D U \end{cases} \tag{1}$$

where the control U is the T_M and T_L, X is variable states include the load speed (ω_L), the motor speed (ω_M), and the shaft torque (T_S), Y is the system output which show the variable states. The system matrixes are:

$$A = \begin{bmatrix} -\frac{B_M}{J_M} & -\frac{1}{J_M} & 0 \\ K_S - \frac{B_M B_S}{J_M} & -B_S(\frac{1}{J_M} + \frac{1}{J_L}) & -(K_S - \frac{B_L B_S}{J_L}) \\ 0 & \frac{1}{J_L} & -\frac{B_L}{J_L} \end{bmatrix} \tag{2}$$

$$B = \begin{bmatrix} \frac{1}{J_M} & \frac{B_S}{J_M} & 0 \\ 0 & \frac{B_S}{J_L} & -\frac{1}{J_L} \end{bmatrix}^T \tag{3}$$

$$C = \begin{bmatrix} 1 & 0 & 0 \\ 0 & 1 & 0 \\ 0 & 0 & 1 \end{bmatrix} \tag{4}$$

$$D = \begin{bmatrix} 0 & 0 & 0 \\ 0 & 0 & 0 \end{bmatrix}^T \tag{5}$$

The load speed and motor speed are:

$$\omega_L(s) = \underbrace{\frac{G_L(s)G_M(s)G_S(s)}{1+G_M(s)G_S(s)+G_L(s)G_S(s)}}_{H_{LM}(s)} T_M(s)$$

$$- \underbrace{\frac{G_L(s)[1+G_M(s)G_S(s)]}{1+G_M(s)G_S(s)+G_L(s)G_S(s)}}_{H_{LL}(s)} T_L(s) \tag{6}$$

$$\omega_M(s) = \underbrace{\frac{G_M(s)[1+G_S(s)G_L(s)]}{1+G_M(s)G_S(s)+G_L(s)G_S(s)}}_{H_{MM}(s)} T_M(s)$$

$$- \underbrace{\frac{G_L(s)G_M(s)G_S(s)}{1+G_M(s)G_S(s)+G_L(s)G_S(s)}}_{H_{ML}(s)} T_L(s) \tag{7}$$

where $G_L(s)$, $G_M(S)$ and $G_S(s)$ are transfer functions of load, motor and shaft, respectively. Fig.2 shows a block diagram representation of the two-mass system. Let a two-input single-output process be represented by the block diagram shown in Fig.3 for which the transfer function is:

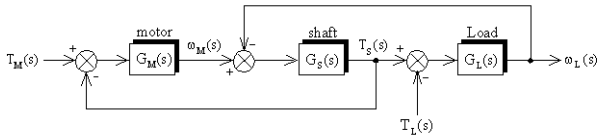

Figure 2. Block diagram of the two-mass system

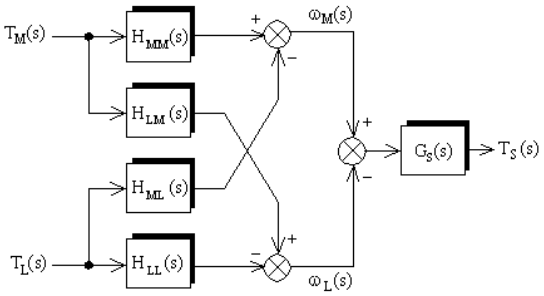

Figure 3. Two-input and single-output of the system

$$\begin{bmatrix} \omega_L \\ \omega_M \end{bmatrix} = \begin{bmatrix} -H_{LL}(s) & H_{LM}(s) \\ -H_{ML}(s) & H_{MM}(s) \end{bmatrix} \begin{bmatrix} T_L \\ T_M \end{bmatrix} \tag{8}$$

where:

$$H_{LL}(s) = \left.\frac{\omega_L(s)}{T_L(s)}\right|_{T_M=0} \tag{9}$$

$$H_{LM}(s) = \left.\frac{\omega_L(s)}{T_M(s)}\right|_{T_L=0} \tag{10}$$

$$H_{MM}(s) = \left.\frac{\omega_M(s)}{T_M(s)}\right|_{T_L=0} \tag{11}$$

$$H_{ML}(s) = \left.\frac{\omega_M(s)}{T_L(s)}\right|_{T_M=0} \tag{12}$$

Open loop transfer function is given by (13), from motor torque to motor speed, is most important in the close loop design.

$$H_{MM}(s) = \frac{1}{J_L J_M} \frac{J_L s^2 + (B_L + B_S)s + K_S}{\Delta(s)} \tag{13}$$

where $\Delta(s)$ is characteristic equation of the open loop system. The viscous damping on most practical machines is low so that the numerator and denominator in (13) are lightly damped.

$$H_{MM}(s) = \frac{1}{J_M} \frac{s^2 + \omega_A^2}{s(s^2 + \omega_R^2)} \tag{14}$$

where the resonance frequency (ω_R) and anti-resonance frequency (ω_A) are defined as:

$$\begin{cases} \omega_R = \sqrt{\dfrac{K_S}{J_L}(1+K_J)} \\ \omega_A = \sqrt{\dfrac{K_S}{J_L}} \end{cases} \tag{15}$$

where K_J is the inertia ratio given by $K_J=J_L/J_M$. Poles and zeros of the two-mass resonant system are placed on imaginary axis. At these frequencies, the phase characteristics change drastically. The natural frequencies are constant, but the excitations change with motor-inverter speed. One important factor has been noticed, in that the resonance characteristics of a two-mass system can be described by its resonance ratio (K_R) which is the quotient of the anti-resonance frequency and resonance frequency of the system:

$$K_R = \frac{\omega_R}{\omega_A} = \sqrt{1+K_J} \tag{16}$$

With $J_M >> J_L$, oscillations of torsional torque are filtered by a large motor inertia J_M and their influence on the control of the motor speed becomes smaller. The direct feedback from the shaft and load speed is very difficult in the industrial application. The load speed ω_L has to be controller according to the commanded speed ω_C, but usually ω_L is not measurable. The measurable output variable is only the motor speed ω_M [3].

III. CONTROL STRATEGY

A block diagram of the speed control system using conventional PID controller [$G_V(s)=K_P+K_I/s+sK_D$] with motor speed feedback is shown in Fig. 4. The motor speed is represented as:

$$\omega_M(s) = \frac{G_V(s)H_{MM}(s)}{1+G_V(s)H_{MM}(s)}\omega_C(s) - \frac{H_{ML}(s)}{1+G_S(s)H_{MM}(s)}T_L(s) \tag{17}$$

When a PID controller is used for two-mass system, the closed-loop transfer function from the speed command ω_C to the motor speed is given by (19):

$$H_C(s) = \frac{\omega_M(s)}{\omega_C(s)} = \frac{(s^2+\omega_A^2)(K_D s^2 + K_P s + K_I)}{\Delta_S(s)} \tag{18}$$

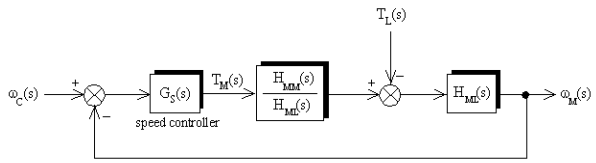

Figure 4. Speed control system using PID controller with motor speed feedback

where $\Delta_S(s)$ is closed-loop characteristic equation and given by:

$$\Delta_S(s) = (K_D+J_M)s^4 + K_P s^3 + (J_M\omega_R^2 + K_I + K_D\omega_A^2)s^2 + K_P\omega_A^2 s + K_I\omega_A^2 \tag{19}$$

The signal flow graph of the two-mass system with a PID controller is shown in Fig.5, where the show coefficient are given by:

$$H_C(s) = \frac{\sum_{k=0}^{k=4} n_k s^k}{\sum_{k=0}^{k=4} d_k s^k} = K_T + \frac{\sum_{k=0}^{k=3} \alpha_k s^k}{\sum_{k=0}^{k=4} \beta_k s^k} \tag{20}$$

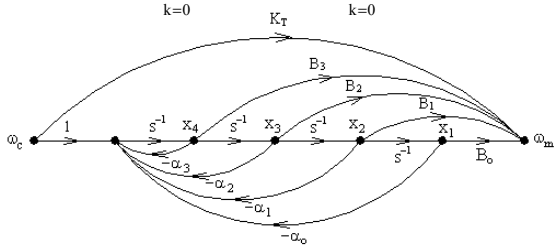

Figure 5. The signal flow graph of the two-mass system

The dynamical equation description of the close loop two-mass system in controllable canonical form realization is:

$$\frac{d}{dt}\begin{bmatrix} x_1 \\ x_2 \\ x_3 \\ x_4 \end{bmatrix} = \begin{bmatrix} 0 & 1 & 0 & 0 \\ 0 & 0 & 1 & 0 \\ 0 & 0 & 0 & 1 \\ -\beta_0 & -\beta_1 & -\beta_2 & -\beta_3 \end{bmatrix}\begin{bmatrix} x_1 \\ x_2 \\ x_3 \\ x_4 \end{bmatrix} + \begin{bmatrix} 0 \\ 0 \\ 0 \\ 1 \end{bmatrix}[\omega_C] \tag{21}$$

$$[\omega_S] = [\alpha_0 \quad \alpha_1 \quad \alpha_2 \quad \alpha_3]\begin{bmatrix} x_1 \\ x_2 \\ x_3 \\ x_4 \end{bmatrix} + [K_T][\omega_C] \tag{22}$$

The closed-loop frequency response is:

$$H_C(j\omega) = \frac{\omega_M(s)}{\omega_C(s)} = \frac{R_{SN}(\omega) + jI_{SN}(\omega)}{R_{SD}(\omega) + jI_{SD}(\omega)} \tag{23}$$

where $R_{SN}(\omega)$ and $I_{SN}(\omega)$ are respectively the real and the imaginary number part of numerator polynomial and $R_{SD}(\omega)$ and $I_{SD}(\omega)$ are respectively the real and the imaginary number part of denominator polynomial of closed loop frequency response:

$$R_{SN}(\omega) = K_I\omega_A^2 - (K_D\omega_A^2 + K_I)\omega^2 + K_D\omega^4 \tag{24}$$

$$R_{SD}(\omega) = (J_M+K_D)\omega^4 - (K_D\omega_A^2 + K_I + J_M\omega_R^2)\omega^2 + K_I\omega_A^2 \tag{25}$$

$$I_{SN}(\omega) = I_{SD}(\omega) = K_P\,(\omega_A^2 - \omega^2)\,\omega \tag{26}$$

From (24) and (25), it can be seen that, for any frequency, $I_{SN}(\omega)$ always equal to $I_{SD}(\omega)$**,** and at frequencies zero and ω_R**,** the absolute values of $R_{SN}(\omega)$ are equal to those of $R_{SD}(\omega)$, so the gain characteristic plot of the closed-loop frequency response crosses the real axis at frequencies zero and ω_R.

IV. DESIGN CONTROLLER

In the coefficient diagram method, there is a relationship among the coefficients of the controlled system closed-loop characteristic polynomial:

$$a_k = \frac{a_o\,\tau^k}{\gamma_{k-1}\,\gamma_{k-2}^2 \cdots\cdots \gamma_1^{k-1}} \tag{27}$$

where τ is the equivalent time constant, γ_k the stability index and k=1, 2, …, n. The polynomial coefficients of characteristic equation (20) are:

$$\begin{cases} K_D + J_M = \dfrac{d_o\,\tau^3}{\gamma_2\,\gamma_1^2} \\ K_P = \dfrac{d_o\,\tau^3}{\gamma_2\,\gamma_1^2} \\ J_M\,\omega_R^2 + K_I + K_D\,\omega_A^2 = \dfrac{d_o\,\tau^2}{\gamma_1} \\ K_P\,\omega_A^2 = d_o\,\tau \end{cases} \tag{28}$$

Finding the solution of (29), the PID controller's gains can be found as following:

$$\begin{cases} K_I = \dfrac{K_S\,\gamma_3}{\gamma_1\,\gamma_2\,\gamma_3 - \gamma_1 - \gamma_3} \\ K_D = \dfrac{J_L\,\gamma_1}{\gamma_1\,\gamma_2\,\gamma_3 - \gamma_1 - \gamma_3} - J_M \\ K_P = \dfrac{\gamma_1\sqrt{K_S\,J_L}\,\sqrt{\gamma_2}}{\gamma_1\,\gamma_2\,\gamma_3 - \gamma_1 - \gamma_3} \end{cases} \tag{29}$$

Also, the value of the equivalent time constant is inversely proportional of that of anti-resonance frequency as:

$$\tau = \frac{\gamma_1\sqrt{\gamma_2}}{\omega_A} \tag{30}$$

V. SIMULATION RESULTS AND DISCUSSIONS

In this section, we verify the validity of the proposed method. All simulation is executed by Matlab. The dominant eigenvalues for open-loop system are P_1=-0.3373 and $P_{2,3}$= -2.9958±j77.2394. The resonant frequency is ω_R=77.3 rad/s and anti-resonant frequency is ω_A=45.2 rad/s. The damping factor of the original plant without the controller is η=0.0284. The step response of speed motor due change in torque motor torque and load torque without PID controller is shown in Fig.6. In this figures, the dashed line and the thick solid line show corresponds relative to motor torque and relative to load torque. Figs. 7 and 8 show the plot of the open-loop frequency response from the motor speed and load speed to the motor torque, respectively.

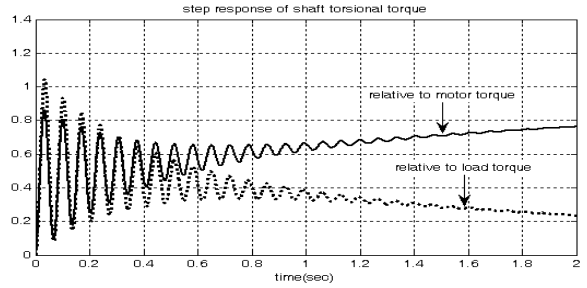

Figure 6. Step response of speed motor

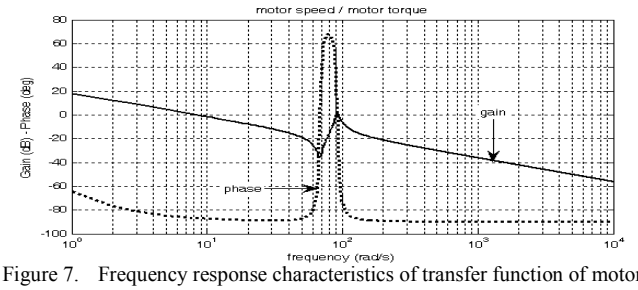

Figure 7. Frequency response characteristics of transfer function of motor torque to motor speed

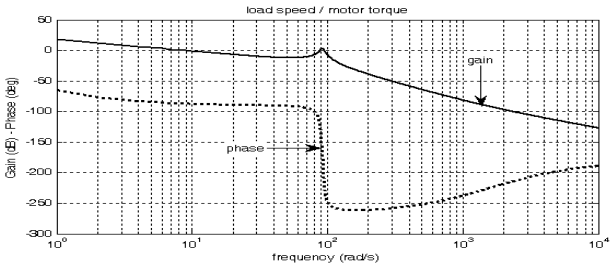

Figure 8. Frequency response characteristics of transfer function of motor torque to load speed

The block diagram representation of the two-mass resonant system with controller in this study is shown in Fig.9. The controller is designed using a PID controller with smaller gains and a feedback proportional compensation of the motor speed. Using the ID control or the PID-P control, the simulation results of the closed-loop frequency response are respectively shown by the solid line and the dash line in Fig. 10. In Figs. 11 and 12, the solid lines show the plots the troque step response of the closed-loop motor speed and shaft with PID-P controller. Also, the break lines show the plots of the motor speed step response with PID controller.

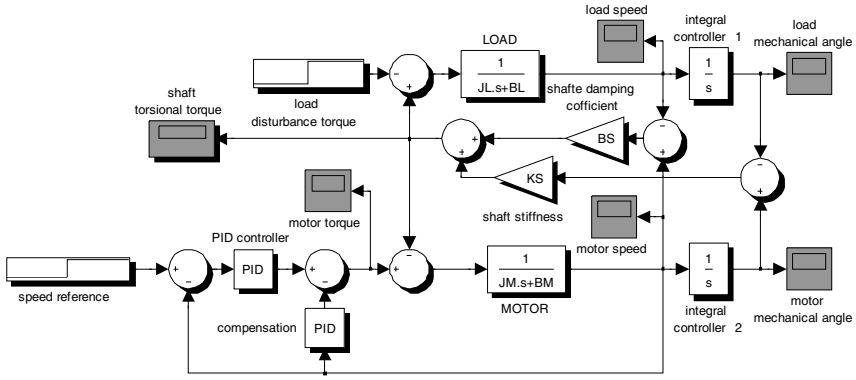

Figure 9. Close-loop model of system in Simulink/Matlab

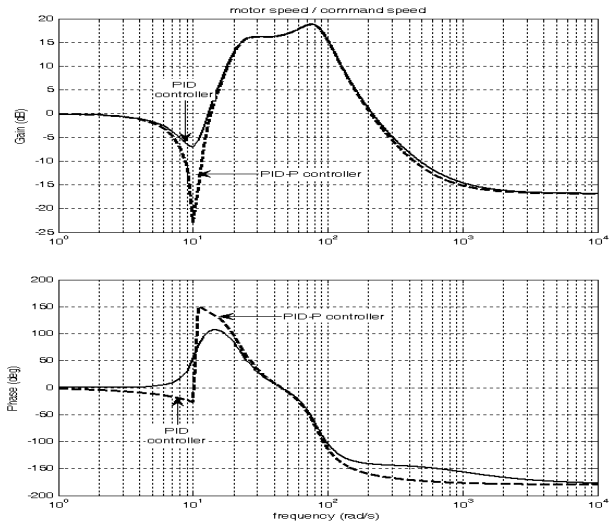

Figure 10. Comparison of the frequency response characteristics

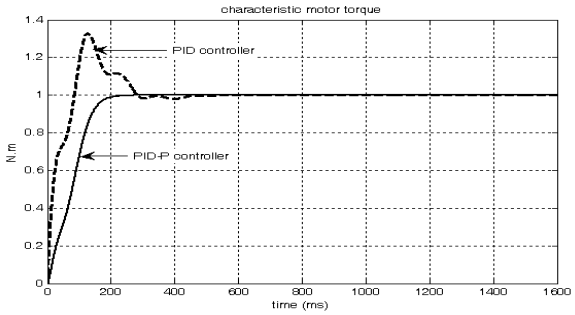

Figure 11. Comparison of the motor speed step response characteristics

VI. ONCLUSION

In this paper, an analysis and design method of the speed control of two-mass resonant system is presented. Analysis and simulation results show that a better speed response to suppress the mechanical vibrations can be got by using the proposed controller.

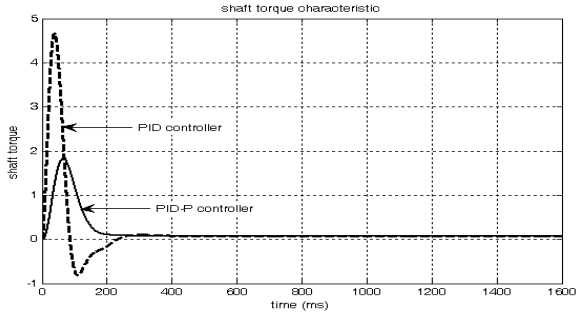

Figure 12. Comparison of the shaft torque step response characteristics

REFERENCES

[1] Y.S.Kim, S.B.Kim, J.S.Kim, C.H.Yoo, H.J.Kim", Two degree of freedom speed control of induction motor having two mass resonant system", IEEE/IECON, Vol.2, pp.1210-1215, Aug. 1996.

[2] K.Sugiura, Y.Hori, "Vibration suppression in 2- and 3-mass system based on the feedback of imperfect derivative of the estimated torsional torque," IEEE Trans. Ind. Electronics, vol. IE-43, No.1, pp.56-64, Feb. 1996.

[3] S.Katsura, K.Ohnishi, "Force servoing by flexible manipulator based on resonance ratio control", IEEE Trans. On Indu. Elec., Vol.54, No.1, pp.539-547, Feb. 2007.

[4] G.Shahgholian, J.Faiz, "An analytical approach to synthesis and modeling of torque control strategy for two-mass resonant systems", Inte. Revi. of Auto. Cont. (IREACO), Vol.2, No.4, pp.459-468, July 2009.

[5] G.Zang, J.Furusho, "Speed control of two-inertia system by PI/PID control," IEEE Trans. Ind. Elec., Vol.47, No.3, pp.603-609, June 2000.

[6] F.Qiao, Q.M.Zhu, S.Y.Li, A.Winfield, "Torsional vibration suppression of a 2-mass main drive system of rolling mill with KF enhanced pole placement", WCICA, pp.206-210, 2002.

[7] S.Morimoto, M.Ohashi, Y.Takeda, K.Tanigchi, "High performance speed control for torsional system based on H_∞ control theory", IEEE/PEDS, Vol.2, pp.828-833, Feb. 1995.

[8] B.Nam, H.Kim, H.Lee, D.Kim, "Optimal speed controller design of the two-inertia stabilization system", PWASET Vol.31, pp.155-160, July 2008.

[9] S.Hashimoto, K.Hara, H.Funato, K.Kamiyama, "AR-based identification and control approach in vibration suppression", IEEE Tran. On Ind. Appl., Vol.37, No.3, pp.806-811, May/June 2001.

[10] J.K.Ji, S.K.Sul, "Kalman filter and LQ Based Speed Controller for Torsional Vibration Suppression in a 2-Mass Motor Drive System," IEEE Trans. Ind. Ele., Vol.IE-43, No.6, pp. 564-571, Dec. 1995.